



## OPEN ACCESS

## EDITED BY

Jiayong Han,  
Shandong Jianzhu University, China

## REVIEWED BY

Yong Niu,  
Shaoxing University, China  
Chao Wang,  
Kunming University of Science and  
Technology, China

## \*CORRESPONDENCE

Jian-Cong Zhang,  
✉ zhang\_jc4@hdec.com  
Shu-Feng Pei,  
✉ peishufeng@ncwu.edu.cn

RECEIVED 29 January 2024

ACCEPTED 28 February 2024

PUBLISHED 14 March 2024

## CITATION

Zhao J-S, Zhang J-C, Pei S-F, Xing L,  
Chen C-F and Zhang G-D (2024),  
Investigation on the failure mechanism of the  
collapse of the columnar jointed basalt in  
underground cavern.  
*Front. Earth Sci.* 12:1378264.  
doi: 10.3389/feart.2024.1378264

## COPYRIGHT

© 2024 Zhao, Zhang, Pei, Xing, Chen and  
Zhang. This is an open-access article  
distributed under the terms of the [Creative  
Commons Attribution License \(CC BY\)](#). The  
use, distribution or reproduction in other  
forums is permitted, provided the original  
author(s) and the copyright owner(s) are  
credited and that the original publication in  
this journal is cited, in accordance with  
accepted academic practice. No use,  
distribution or reproduction is permitted  
which does not comply with these terms.

# Investigation on the failure mechanism of the collapse of the columnar jointed basalt in underground cavern

Jin-Shuai Zhao<sup>1,2,3</sup>, Jian-Cong Zhang<sup>1\*</sup>, Shu-Feng Pei<sup>4\*</sup>,  
Liang Xing<sup>5</sup>, Chong-Feng Chen<sup>6</sup> and Guang-Duan Zhang<sup>7</sup>

<sup>1</sup>PowerChina Huadong Engineering Corporation Limited, Hangzhou, China, <sup>2</sup>Faculty of Civil Engineering and Mechanics, Jiangsu University, Zhenjiang, China, <sup>3</sup>Key Laboratory of Geotechnical Mechanics and Engineering of Ministry of Water Resources, Yangtze River Scientific Research Institute, Wuhan, China, <sup>4</sup>North China University of Water Resources and Electric Power, Zhengzhou, China, <sup>5</sup>Guangdong Provincial Academy of Building Research Group Corporation Limited, Guangzhou, China, <sup>6</sup>Xi'an Research Institute, China Coal Technology and Engineering Group Corporation, Xi'an, China, <sup>7</sup>Heze Mudan District Natural Resources Bureau, Heze, China

Columnar jointed basalt (CJB) is a kind of jointed rock with a polygonal cylinder mosaic structure that has complex mechanical properties such as discontinuity and heterogeneity. The typical geological structure of the CJB is the intercolumnar joint plane and the implicit joint plane, which obviously affect the mechanical properties of the rock mass. Controlling the unloading relaxation of the CJB is a key problem during the construction of underground engineering. In this paper, *in-situ* acoustic wave and panoramic borehole camera measurements were carried out in the cavern of the Baihetan project to understand the failure mechanism of the collapse of the CJB. It was quite clear that the evolution of the excavation damage zone (EDZ) of the CJB depends on the time and spatial effects. The closer to the collapse zone, the greater the degree of relaxation failure of the columnar joint rock mass; the further away from the cavern perimeter, the more stable the surrounding rock. The correction between wave velocity and cracks in the rock mass was also discussed. This field test and theoretical analysis can provide a reference for studying the failure mechanism and control measures of CJB in underground caverns under high geostress.

## KEYWORDS

columnar jointed basalt, underground cavern, collapse mechanism, mechanical properties, rock fracture

## 1 Introduction

The columnar joint is a common primary fracture structure in basalt (Hoek and Brown, 1980; Jiang et al., 2014; Shi et al., 2020; Zhao et al., 2022a; b). Columnar joints are formed by cooling shrinkage during diagenesis and are more common in thick lavas (Schultz, 1995; Almqvist et al., 2012; Jiang et al., 2019; Liu et al., 2023). Columnar joints divide the rock mass into regular polygonal long columns, essentially perpendicular to the lava plane. As a type of dense jointed rock with a regular planar network structure, columnar jointed rock has complex mechanical response processes under high

geostress, such as joint surface opening, rock block fracture and relaxation failure (Brady and Brown, 2005; Xia et al., 2020; 2023; 2024; Hu et al., 2023; Zheng et al., 2023a; b; Si et al., 2024a; b; Wang et al., 2024). Given the weak and complex mechanical properties of columnar joints, it is easy to induce failures during the excavation of the CJB in underground caverns (Hao et al., 2016; 2021; 2022; Li et al., 2020; 2023; Zhao et al., 2023).

Structural planes such as joints, fissures and faults are common in rock materials (Saliba and Jagla, 2003; Li et al., 2021; 2022; 2024; Zhang et al., 2022). The structural plane is the most important factor in controlling the deformation, strength and permeability of the surrounding rock of the tunnel (Smith and Holden, 2021; Cai et al., 2022a; b, 2023; Guo et al., 2023a; b; Xu et al., 2024; Lu et al., 2024). The structural plane derives the complex properties such as anisotropy and heterogeneity of the surrounding rock, which makes the mechanical behavior of the rock mass much more complex than that of general homogeneous, continuous and isotropic materials (Jin et al., 2014; Xia et al., 2020; Lei et al., 2023; Chen et al., 2024; Zhao et al., 2024a; Zhao et al., 2024b). In essence, the fracture of the CJB is a three-dimensional evolutionary process (Feng et al., 2021; Yang et al., 2021; Deng et al., 2023). To fully understand the mechanical property of rock fracture, high-precision microseismic (MS) monitoring technology is introduced into underground caverns to monitor the fracture process of the CJB (Chen et al., 2014; Han et al., 2023). The 3D fracture process of the CJB under strong excavation unloading, in particular the time-dependent relaxation and spatial heterogeneity, has been successfully revealed by MS monitoring (Feng et al., 2015). In short, the MS monitoring technology can effectively resolve the basic spatiotemporal characteristics of the microseismicity of the CJB in caverns.

To investigate the relaxation characteristics and failure mechanism of the collapse of the CJB, acoustic velocity measurements and a panoramic borehole camera were carried out in the underground cavern. The results presented in this paper provide an indication of the excavation induced mechanical response of the CJB.



FIGURE 1  
Aerial view of the Baihetan project in the Jinsha River, China.

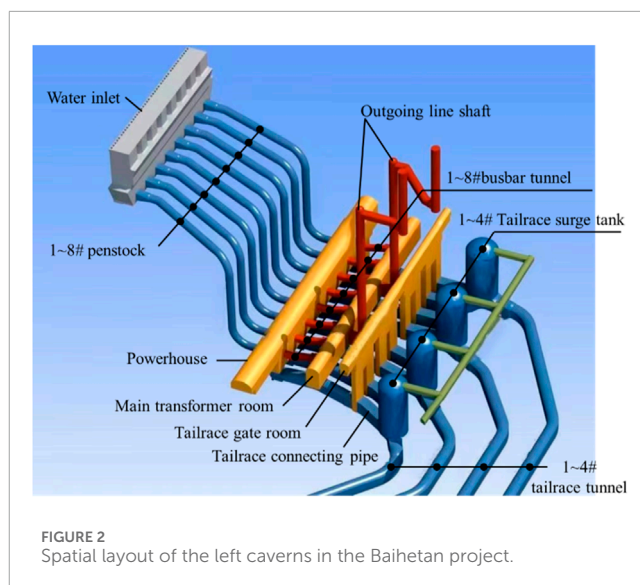


FIGURE 2  
Spatial layout of the left caverns in the Baihetan project.

## 2 Project background

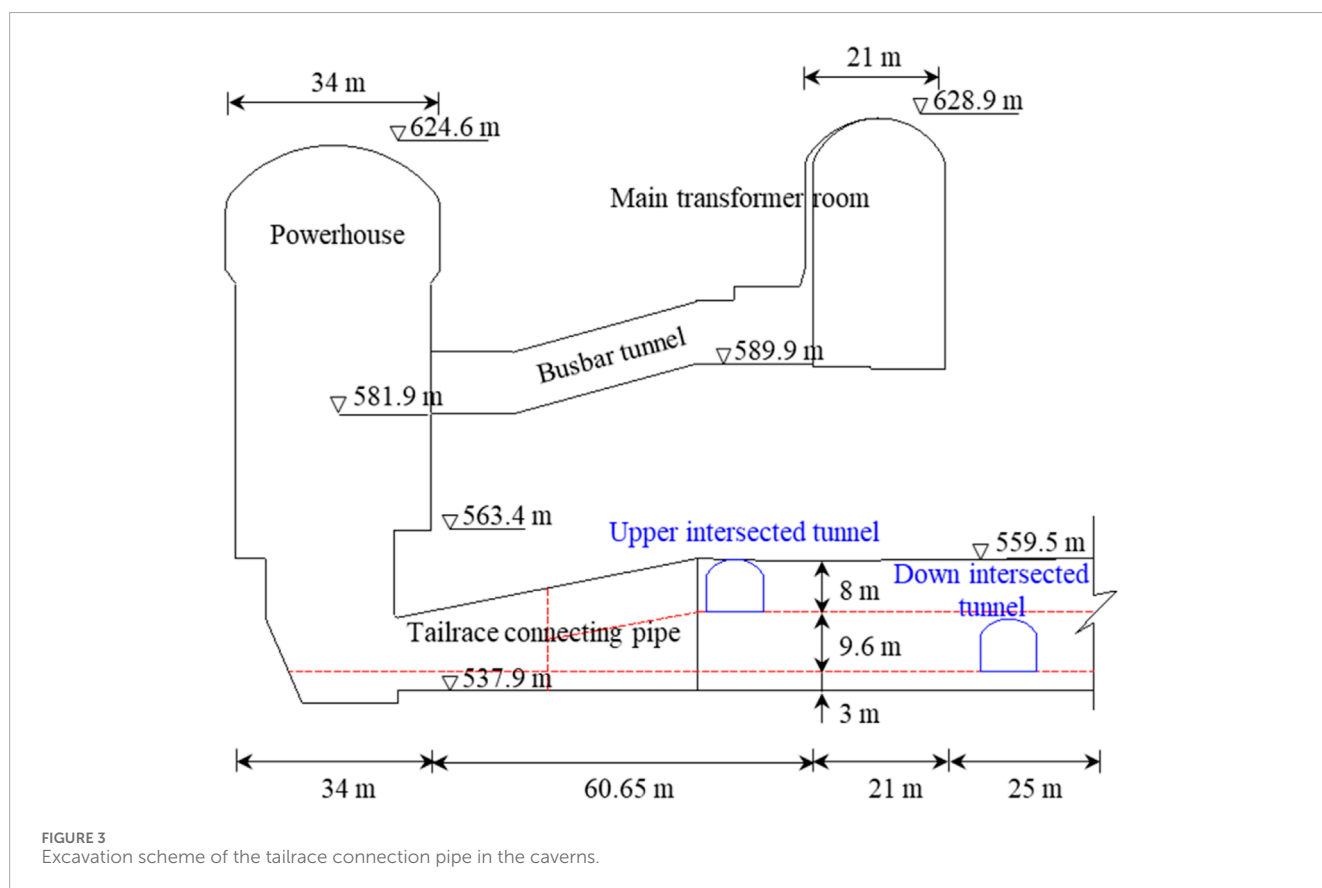
### 2.1 Project introduction

The aerial view of the Baihetan project is shown in Figure 1. The hydropower project is equipped with eight sets of hydropower generating units on both the left and right banks. The capacity of each hydropower generator of the project is 1000 MW. The total excavation length and volume of the underground cavern groups are 217 km and 25 million m<sup>3</sup>, respectively. The concrete dam of the project is designed as a double curved dam, which is located in an asymmetrical valley in the V shape.

The spatial layout of the left cavern groups of the Baihetan project is exhibited in Figure 2. The four large caverns, namely, the powerhouse, the tailrace surge tank, the main transformer room and the tailrace gate room, are arranged parallel to each other. The busbar tunnels and the tailrace connection pipes are arranged perpendicular to the axis of the powerhouse.

### 2.2 Geological information

The columnar jointed basalts of the Baihetan project are developed in several rock flow layers, and the columnar jointed basalts of the P<sub>2</sub>β<sub>2</sub><sup>3</sup> layer are exposed in the tailrace connection pipes. Depending on the diameter and length of the column, the Baihetan columnar jointed basalts can be divided into three categories: small, medium and large columnar jointed basalts. The small columnar jointed basalt is 13–25 cm in diameter, and 2–3 m in length. The micro-cracks are developed, and the length of the cut block is about 5 cm. The diameter of the medium columnar jointed basalt is 25–50 cm, and the length of the column is generally 0.5–2.0 m. The internal micro-cracks are developed, but the mutual occlusion is not completely cut off, and the block size is about 10 cm. The large columnar jointed basalt has a diameter of 0.5–2.5 m and a length of 1.5–5 m.



### 2.3 Excavation scheme

The tailrace connection pipes are located between the powerhouse and the tailrace surge tank. The axis of the tailrace connection pipe is perpendicular to the axis of the powerhouse. There are a total of eight tailrace connection pipes, which are arranged approximately in parallel with equal spacing of 38 m. The sectional shape of the tailrace connection pipe is a straight wall and semi-circular arch. The width and the height of the tailrace connection pipe are 16.0 and 20.6 m, respectively. Therefore, the tailrace connection pipes adopt a layered excavation scheme along the elevation direction. The specific excavation scheme of the tailrace connection pipe is shown in Figure 3. The tailrace connection pipe is divided into three layers along the elevation direction, and the excavation heights of each layer are 8, 9.6 and 3.0 m, respectively. The layer excavation boundary of the tailrace connection pipe is indicated by the red dashed line in Figure 3.

## 3 Collapse mechanism of the CJB

### 3.1 Characteristics of collapse

During the excavation of the cavern, a large scale collapse of the rock mass occurred in the sidewalls of the No. 5 tailrace connection pipe. The depth of the collapsed area is approximately 1.5 m, and

the extent of the collapse failure is very severe (Figure 4). The site investigation shows that the CJB was developed in this region. The collapse area is close to the working face and the vibration damage to the CJB in this area is severe under the influence of the blast disturbance. In addition, only steel mesh and shotcrete support is used after excavation and no effective reinforcement measures, such as systematic bolting and anchoring cables, are adopted to control the relaxation failure of the CJB. This is another important reason for the collapse of the surrounding rock in this area.

### 3.2 Geological analysis

The geological survey reveals that the typical CJB exposed in the tailrace connection pipes is shown in Figure 5. The cross section of the CJB is irregular polygon, mainly pentagon and hexagon. The edge length of the irregular polygon is in the range of 10–25 cm, and the axis inclination of the CJB is about 75° ~ 85° (Figure 5A). The intercolumnar joint plane, formed by condensation shrinkage of the basalt, is the main structural plane of the CJB. The intercolumnar joint plane is covered with a chlorite film and has an oily sheen. In addition to the intercolumnar joint plane, there are a large number of implicit joint planes in the CJB (Figure 5B). Note that, depending on the occurrence of joints, the implicit joints developed in the column are mainly steeply inclined implicit joints and gently inclined implicit joints.

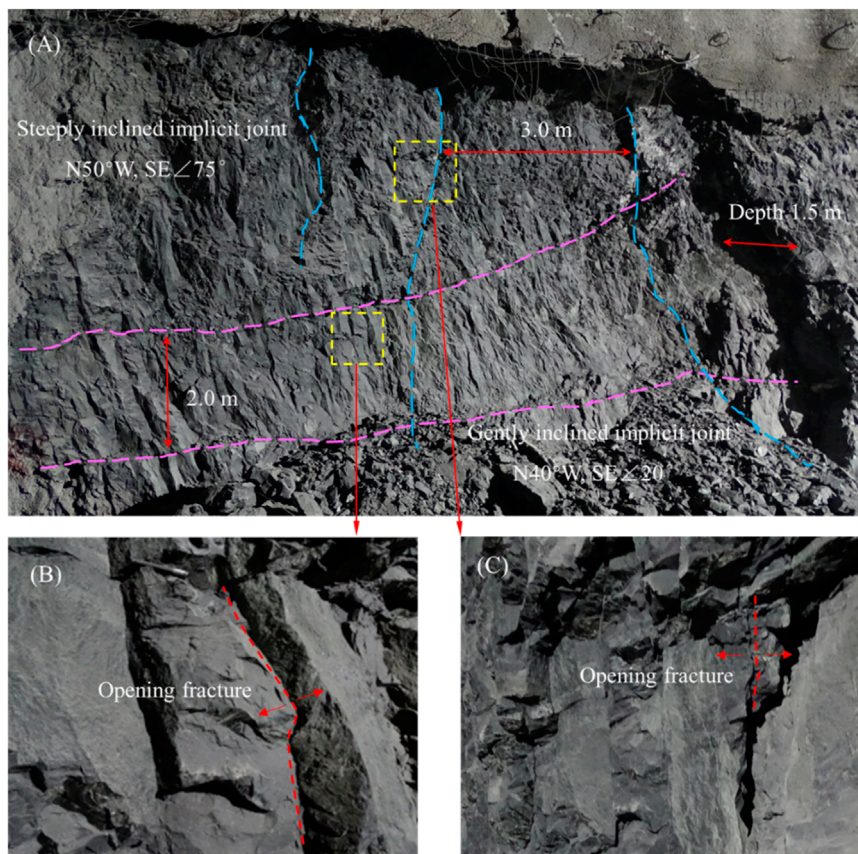


**FIGURE 4** Collapse of the columnar jointed basalt. (A) geological of the collapse zone, (B) opening failure of the intercolumnar joint plane, (C) fracture of the implicit joint plane.

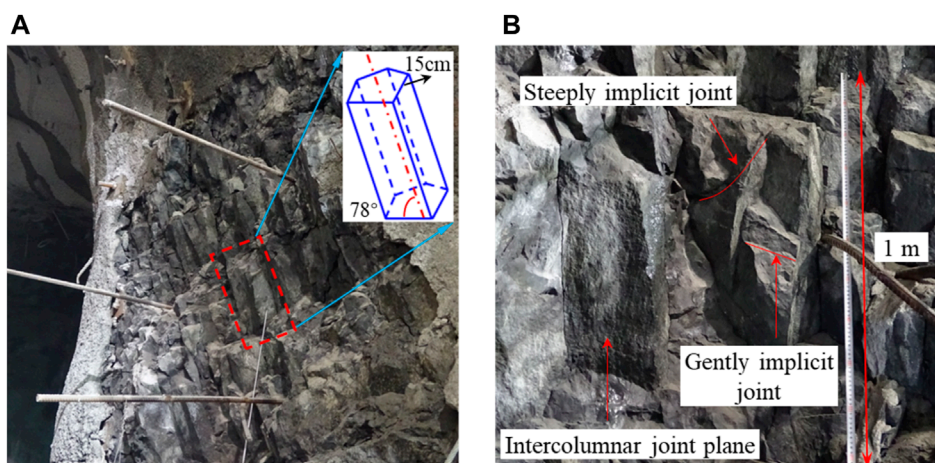


**FIGURE 5** Typical characteristic of the columnar jointed basalt exposed in the cavern. (A) irregular polygon, (B) intercolumnar and implicit joint planes.

In the stress compression state, the internal joints of the rock are tightly closed and embedded, and the mechanical performance of the rock mass is good. However, the stress is adjusted and

redistributed after excavation and unloading. It has been found that the material discontinuity of the structural plane has a significant influence on the failure mode of the rock mass during cavern

excavation. The joint surface between the columns slowly opens after the confining pressure is released (Figure 4B). The implicit joints in the column then rupture (Figure 4C). Failure of the joint plane, such as opening and sliding during excavation unloading, results in a significant reduction in the mechanical strength of the CJB. Under the action of unfavorable geological conditions and excavation unloading, the CJB relaxes, resulting in deformation and collapse to the air face.

### 3.3 Acoustic measurement

#### 3.3.1 Layout of boreholes

An *in-situ* acoustic wave measurement was carried out in the No. 5 tailrace connection pipe to deeply detect and reveal the failure mechanism of the collapse of the columnar jointed basalt under blast disturbance. Four acoustic boreholes were drilled in the sidewalls near the collapse area of the No. 5 tailrace connection pipe. The specific layout of the acoustic boreholes is shown in Figure 6. From the left to the right sidewall of the No. 5 tailrace connection pipe, the acoustic boreholes are labelled D1, D2, D3, and D4, respectively. These boreholes are arranged parallel to each other, and the distance between the adjacent boreholes is 1 m. The length of these boreholes is 8 m.

#### 3.3.2 Relaxation characteristics

Excavation-induced unloading relaxation characteristics of the rock mass can be reflected by the acoustic wave testing. In order to study the temporal evolution of the relaxation characteristics of the CJB, multiple acoustic tests were carried out in the collapse area of the No. 5 tailrace connection pipe. The criterion for assessing the relaxation depth of the rock mass is the apparent inflection point of the acoustic velocity (Feng et al., 2016). It is clearly shown that the acoustic velocity of the relaxation zone is less than 3,500 m/s, displaying that the relaxation fracture of the surrounding rock is severe in this part of the area (Figure 7). The acoustic velocity is related to the lithology, rigidity and integrity of the rock mass. It is therefore concluded that the micro-cracks and fractures in the relaxation zone are open. The acoustic velocity of the surrounding rock in the deeper zone away from the free face is approximately 5,500 m/s, indicating that the surrounding rock in this area is relatively intact. Notably, there is a localised zone of acoustic velocity decrease in the surrounding rock, which drops to approximately 4,200 m/s (Figures 7C, D). In fact, the surrounding rock in the deeper part of the borehole is in a three-dimensional compressional state and the rapid decrease in acoustic velocity indicates that there is a micro-crack zone in this area. The results of multiple acoustic wave measurements show that the relaxation depth of the CJB gradually increases with time. The acoustic velocity of the rock mass also decreases with time. It is quite clear that the evolution of the unloading relaxation of the CJB is dependent on the effect of time. Therefore, timely and effective placement of support reinforcement after excavation is of great importance to control the growth of the relaxation depth of the CJB.

The temporal evolution of the excavation damage zone of the CJB in the No.5 tailrace connection pipe is shown in Figure 8. The EDZs of the No.5 tailrace connection pipe are in the range of 1.8–2.4 m. Obviously, the measured excavation damage zone of

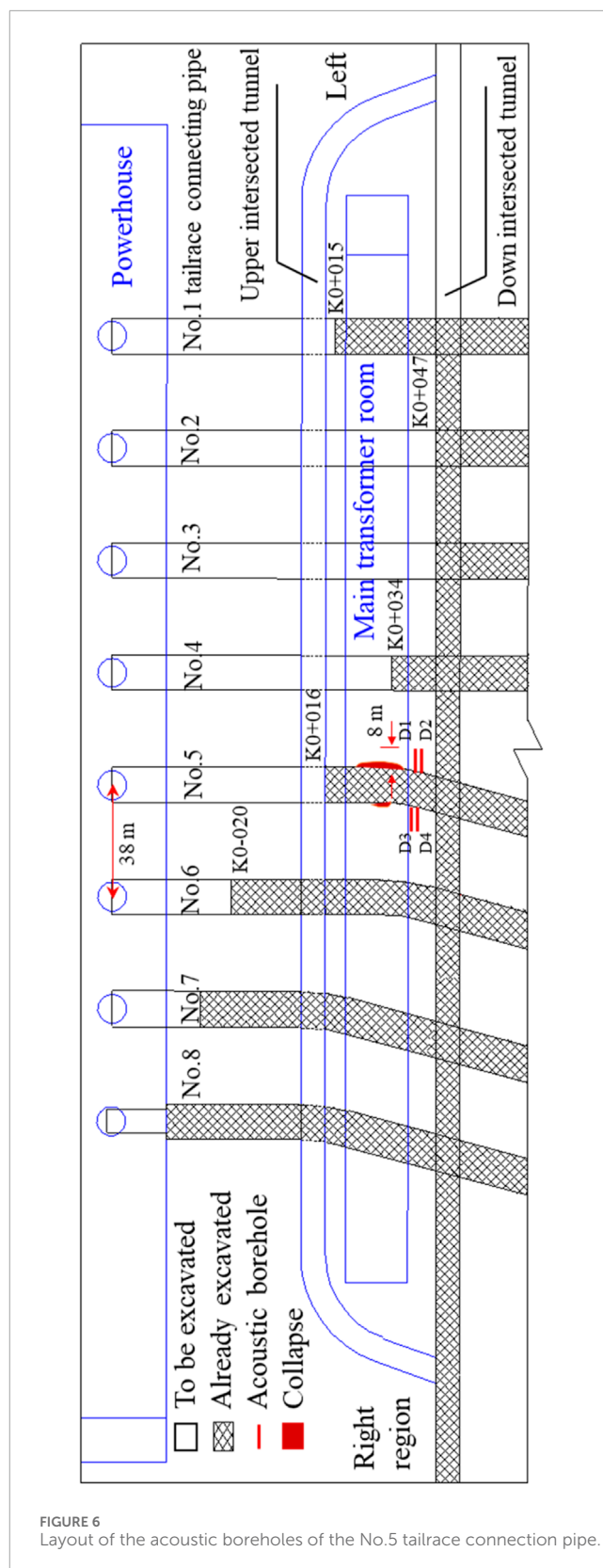
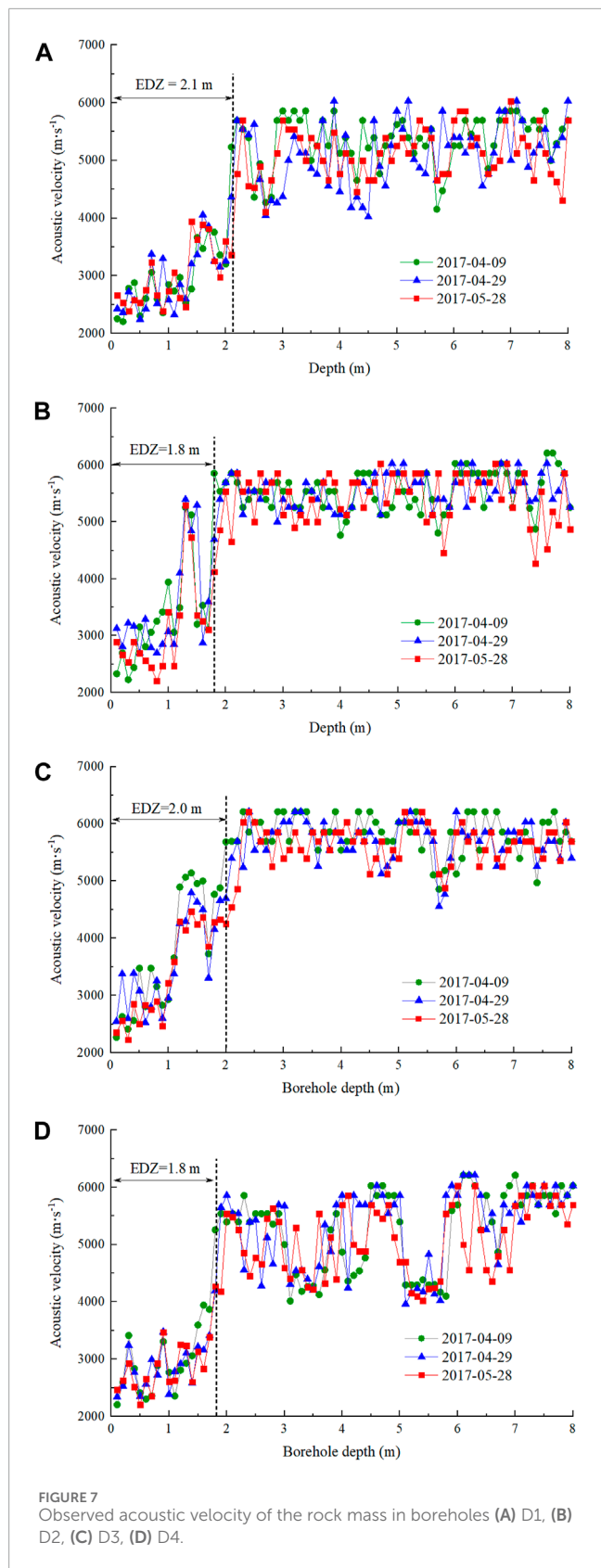
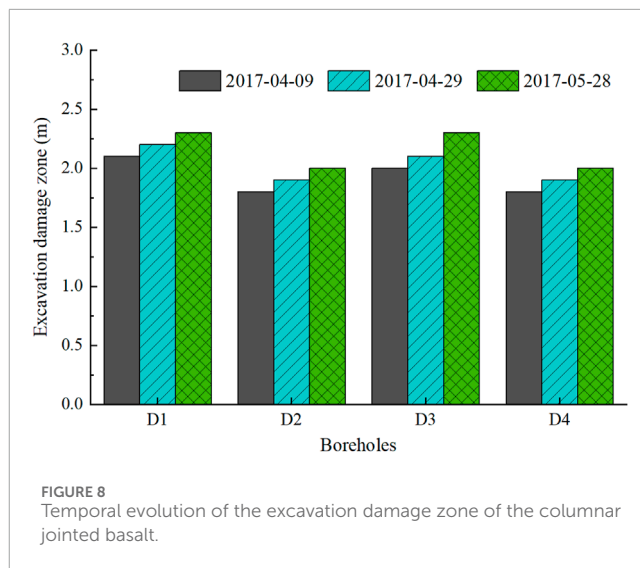


FIGURE 6  
Layout of the acoustic boreholes of the No.5 tailrace connection pipe.

the borehole near the collapse area (D1 and D3) is greater than that of the borehole away from the collapse area (D2 and D4). The maximum excavation damage zone of the boreholes near and far from the collapse area is 2.4 and 2.1 m, respectively. And the



minimum excavation damage zone of the boreholes near and far from the collapse area is 2.0 and 1.8 m, respectively. Therefore, the development of the excavation damage zone of the CJB also depends on the spatial effect. In other words, the closer to the collapse zone,



the greater the degree of relaxation failure of the CJB; the further away from the cavern perimeter, the more stable the rock mass.

### 3.4 Panoramic borehole camera

In order to study the internal joints in the EDZ of the surrounding rock more intuitively, the crack characteristics of the CJB were observed using the panoramic borehole camera. Typical test results from a borehole camera are shown in Figure 9. The observation results display that there are a large number of joints or macroscopic fractures in the region of 0–1 m from the cavern perimeter, illustrating that the integrity of the CJB is very poor. The widths of these macroscopic fractures are 1–3 cm, with a maximum of 5 cm. The fracture planes extend to a depth of 2 m from the cavern perimeter, indicating that stress relaxation and fracturing of the rock mass is severe. Macroscopic cracks with a width of 2–8 cm are also distributed in the deeper part of the surrounding rock. In addition, a large number of implicit joints are developed in the region of 4–8 m from the cavern perimeter, declaring that the lithology of the CJB as a whole is poor.

In the absence of excavation disturbance, the implicit joints are in a closed state and the rock mass shows no obvious damage. However, the typical geological structure such as the intercolumnar joint plane and the implicit joint plane are developed in the CJB. These discontinuous geological structure not only reduces the integrity of the rock mass, but also affect the mechanical properties of the rock mass. Therefore, under the action of excavation unloading or external force disturbance, the CJB has a potential risk of large-scale unloading relaxation damage. Under the disturbance of excavation unloading, the joint surface between the columns tends to relax and open, forming macroscopic cracks and increasing the risk of collapse failure of the rock mass. In addition, the borehole camera results show that the internal joint surface and cracks are more developed and the cracks cut through the rock mass, resulting in poor overall integrity of the surrounding rock of the CJB (Muller, 1998; Antonellini and Mollema, 2019). This is also the reason why the shallow surrounding rock of the cavern is prone to collapse after mining of the CJB.

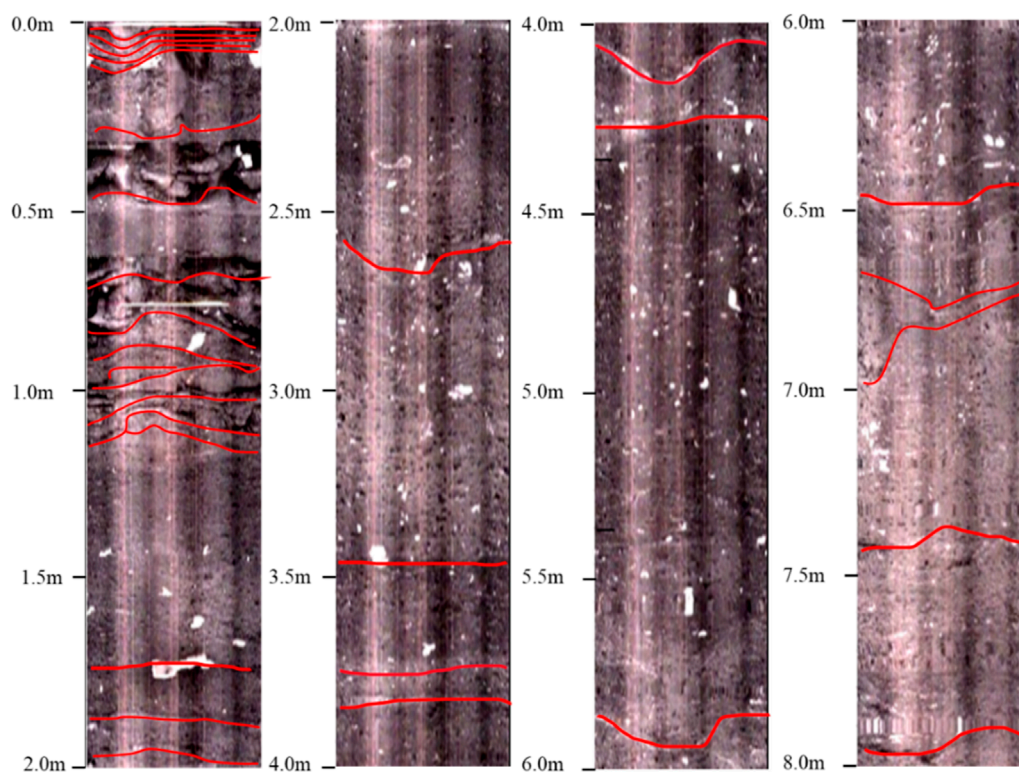


FIGURE 9 Results of borehole camera observations of the columnar jointed basalt.

## 4 Discussion

### 4.1 Correlation between acoustic velocity and cracks

A comparison between the acoustic velocity results and the cracks in the CJB is indicated in Figure 10. The acoustic test shows that the velocity of the CJB in the shallow range of 0–1 m from the cavern perimeter is significantly reduced by excavation unloading, and the average wave velocity is reduced to 2,500 m/s. The average velocity of the rock in the 1–2 m range increases to 4,200 m/s and it is speculated that the quality or integrity of the rock in this area is slightly better than that in the 0–1 m range. The panoramic borehole camera shows that many cracks are developed in the range of 0–1 m from the cavern perimeter, and breakouts are also observed in the borehole. With respect to the range of 0–1 m, the number and size of cracks in the range of 1–2 m are significantly reduced. It is worth noting that the wave velocity of the rock mass drops sharply at a depth of approximately 4.4 m, corresponding to a distinct fracture observed by the borehole camera (see star in Figure 10). The same feature is found at a depth of approximately 5.8 m from the cavern perimeter. Therefore, comparative analysis of the borehole camera and acoustic test shows that the variation in wave velocity is consistent with the distribution of cracks. In other words, the velocity of the surrounding rock is significantly reduced in the area where the cracks are densely developed.

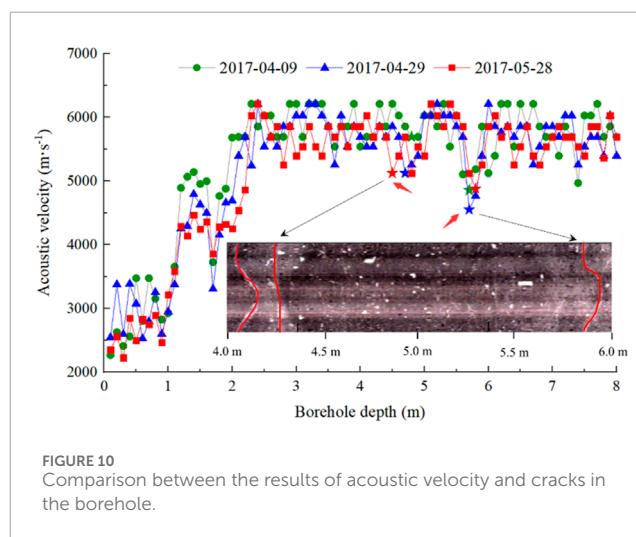
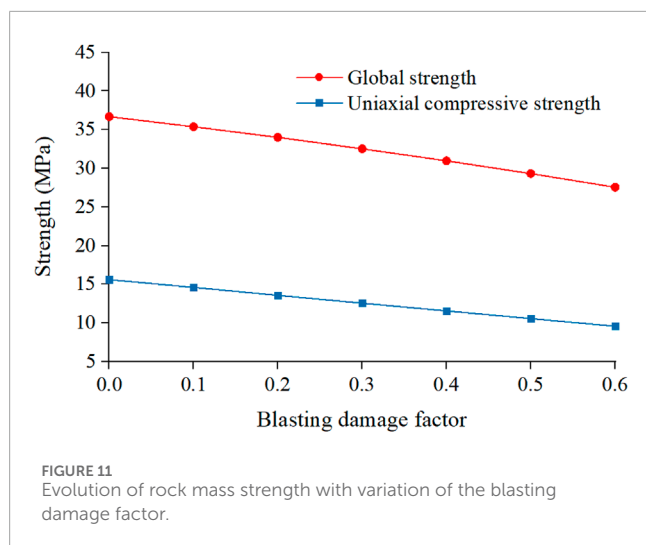


FIGURE 10 Comparison between the results of acoustic velocity and cracks in the borehole.

### 4.2 Strength of the CJB

The strength of the rock mass is closely related to the quality of the rock. The main basis for assessing rock quality is the structural characteristics and the structure plane state of the rock mass. The physical and mechanical properties of jointed rock can be quantitatively characterised by the Hoek-Brown criterion. And the computational formula of the criterion is as shown in Eqs. 1–4



(Martin et al., 1999):

$$\sigma_1 = \sigma_3 + \sigma_c \left( m_b \frac{\sigma_3}{\sigma_c} + s \right)^a \quad (1)$$

$$m_b = m_i \exp\left(\frac{GSI - 100}{28 - 14D}\right) \quad (2)$$

$$s = \exp\left(\frac{GSI - 100}{9 - 3D}\right) \quad (3)$$

$$a = \frac{1}{2} + \frac{1}{6} \left( \exp\left(-\frac{GSI}{15}\right) - \exp\left(-\frac{20}{3}\right) \right) \quad (4)$$

Where  $\sigma_c$  is the uniaxial compressive strength of the intact rock;  $m_i$  is the rock material constant;  $m_b$ ,  $s$ , and  $a$  are the empirical parameters of the Hoek-Brown criteria;  $GSI$  is the geological strength index;  $D$  is the blasting damage factor.

The Geological Strength Index (GSI) is a quantitative index for assessing the strength of the rock mass (Hoek et al., 1998). As an important parameter of the Hoek-Brown criterion, GSI realises the quantitative calculation of the rock mass strength. The rock mass parameters of the CJB under blasting excavation can be calculated using the RocLab software (Hoek and Brown, 1988), as shown in Figure 11. It is evident that the global strength and the uniaxial compressive strength of the field rock mass have an approximately negative linear correlation with the blast damage factor. As the blast damage factor increases, the global strength and uniaxial compressive strength of the field rock mass progressively decrease. For every 0.1 increase in the blast damage factor, the strength of the rock mass is reduced by approximately 4%–7%.

The rock structure of the CJB is a mosaic structure. Prior to excavation, the structure of the rock is tightly compacted and the mechanical properties are good, whereas after excavation the mechanical properties decrease sharply. Therefore, on the one hand, short footages and small charges should be used in blasting excavation to reduce the degree of deterioration and damage to the CJB. On the other hand, rock bolts and anchor cables should be used to strengthen the rock and prevent secondary damage.

## 5 Conclusion

In this paper, *in-situ* acoustic wave velocity and borehole camera tests were carried out to investigate the collapse of the CJB in the tailrace connection pipe of the Baihetan hydropower station, China. The failure mechanism of the collapse of the CJB was systematically investigated, and the main conclusions are listed as below.

The panoramic borehole camera results show that the joints in the CJB of the tailrace connection pipes are densely developed, and the relaxation and joint surface opening behaviour after excavation unloading is evident. And the mechanical properties of the CJB show a clear spatiotemporal effect under the influence of the unloading of the excavation. The results of the continuous field observations show that the excavation damage zones of the CJB increase slowly, i.e., the unloading relaxation of the CJB is a time-dependent failure process. The development of the excavation damage zone of the CJB also depends on the spatial effect. That is, the closer to the collapse zone, the greater the degree of relaxation failure of the CJB; the further away from the cavern perimeter, the more stable the rock mass.

As the cavern is excavated and unloaded, the intercolumnar joint plane and the implicit joint planes of the CJB gradually open. CJB is prone to collapse under the action of external forces, posing a serious threat to the safety of mechanical equipment and construction personnel. The research results in this paper can provide a reference for studying the failure mechanism and control measures of CJB. In other words, how to effectively prevent the opening and fracturing of the joint plane is the key to preventing the failure of the CJB of the cavern.

## Data availability statement

The original contributions presented in the study are included in the article/Supplementary material, further inquiries can be directed to the corresponding authors.

## Author contributions

J-SZ: Writing–review and editing, Writing–original draft, Resources, Methodology, Funding acquisition, Data curation. J-CZ: Writing–review and editing, Formal Analysis. S-FP: Writing–review and editing, Methodology. LX: Writing–original draft, Validation, Supervision. C-FC: Writing–original draft, Methodology, Investigation. G-DZ: Writing–original draft, Methodology, Investigation.

## Funding

The author(s) declare financial support was received for the research, authorship, and/or publication of this article. This research is supported by the National Natural Science Foundation of China (52209132), China Postdoctoral Science Foundation (2023M733317) and the CRSRI Open Research Program (Program SN: CKWV20231173/KY).

## Acknowledgments

The authors would like to thank Prof. Xia-Ting Feng for his help with the *in-situ* measurements using acoustic waves and the panoramic borehole camera.

## Conflict of interest

Authors J-SZ and J-CZ were employed by PowerChina Huadong Engineering Corporation Limited. Author LX was employed by Guangdong Provincial Academy of Building Research Group Corporation Limited. Author C-FC was employed by China Coal Technology and Engineering Group Corporation.

## References

- Almqvist, B. S. G., Bosshard, S. A., Hirt, A. M., Mattsson, H. B., and Hetényi, G. (2012). Internal flow structures in columnar jointed basalt from Hrepphólar, Iceland: II. Magnetic anisotropy and rock magnetic properties. *B. Volcanol.* 74, 1667–1681. doi:10.1007/s00445-012-0622-0
- Antonellini, M., and Mollema, P. N. (2019). Outcrop fracture network characterization for unraveling deformation sequence, geomechanical properties distribution, and slope stability in a flysch sequence (Monte Venere Formation, Northern Apennines, Italy). *Int. J. Earth Sci.* 108, 735–751. doi:10.1007/s00531-019-01685-y
- Brady, B.-H.-G., and Brown, E.-T. (2005). *Rock mechanics for underground mining*. New York: Kluwer Academic Publishers.
- Cai, W., Zhu, H., and Liang, W. (2022a). Three-dimensional stress rotation and control mechanism of deep tunneling incorporating generalized Zhang–Zhu strength-based forward analysis. *Eng. Geol.* 308, 106806. doi:10.1016/j.enggeo.2022.106806
- Cai, W., Zhu, H., and Liang, W. (2022b). Three-dimensional tunnel face extrusion and reinforcement effects of underground excavations in deep rock masses. *Int. J. Rock Mech. Min. Sci.* 150, 104999. doi:10.1016/j.ijrmms.2021.104999
- Cai, W., Zhu, H., Liang, W., Vu, B., and Wu, W. (2023). Physical and numerical investigation on nonlinear mechanical properties of deep-buried rock tunnel excavation unloading under complicated ground stresses. *Tunn. Undergr. Sp. Tech.* 138, 105197. doi:10.1016/j.tust.2023.105197
- Chen, B.-R., Li, Q.-P., Feng, X.-T., Xiao, Y.-X., Feng, G.-L., and Hu, L.-X. (2014). Microseismic monitoring of columnar jointed basalt fracture activity: a trial at the Baihetan Hydropower Station, China. *J. Seismol.* 18, 773–793. doi:10.1007/s10950-014-9445-0
- Chen, J., Hu, T., Hu, X., and Jia, K. (2024). Study on the influence of crack depth on the safety of tunnel lining structure. *Tunn. Undergr. Sp. Technol.* 143, 105470. doi:10.1016/j.tust.2023.105470
- Deng, Z., Pan, M., Niu, J., Jiang, S., Wu, B., and Li, S. (2023). Spatial prediction of rockhead profile using the Gaussian process regression method. *Can. Geotech. J.* 60, 1849–1860. doi:10.1139/cgj-2022-0372
- Feng, G., Feng, X., and Chen, B. (2015). Temporal-spatial characteristics of microseismic activity in columnar jointed basalt in tunnelling at Baihetan hydropower station. *Chin. J. Rock Mech. Eng.* 34, 1967–1975. (in Chinese). doi:10.13722/j.cnki.jrme.2013.1860
- Feng, G., Zhang, J., Jiang, Q., Li, S., Xiao, Y., and Yao, Z. (2021). Synergistic observation and mechanism analysis of time-dependent fracture process of columnar jointed rockmass under strong unloading during excavation. *Chin. J. Rock Mech. Eng.* 40, 3041–3051. (in Chinese). doi:10.13722/j.cnki.jrme.2021.0200
- Feng, X. T., Hao, X., Jiang, Q., Li, S., and Hudson, J. A. (2016). Rock cracking indices for improved tunnel support design: a case study for columnar jointed rock masses. *Rock Mech. Rock. Eng.* 49, 2115–2130. doi:10.1007/s00603-015-0903-y
- Guo, H., Sun, Q., Feng, G., Li, S., and Xiao, Y. (2023a). *In-situ* observations of damage-fracture evolution in surrounding rock upon unloading in 2400-m-deep tunnels. *Int. J. Min. Sci. Technol.* 33, 437–446. doi:10.1016/j.ijmst.2022.11.008
- Guo, Y., Luo, L., Ma, R., Li, S., Zhang, W., and Wang, C. (2023b). Study on surface deformation and movement caused by deep continuous mining of steeply inclined ore bodies. *Sustainability* 15, 11815. doi:10.3390/su151511815
- Han, J., Wang, J., Jia, D., Yan, F., Zhao, Y., Bai, X., et al. (2023). Construction technologies and mechanical effects of the pipe-jacking crossing anchor-cable group in soft stratum. *Front. Earth Sci.* 10, 1019801. doi:10.3389/feart.2022.1019801
- Hao, X., Feng, X., Yang, C., Jiang, Q., and Li, S. J. (2016). Analysis of EDZ development of columnar jointed rock mass in the Baihetan diversion tunnel. *Rock Mech. Rock. Eng.* 49, 1289–1312. doi:10.1007/s00603-015-0829-4
- Hao, X., Yuan, L., Sun, Z., Zhao, Y., Ren, B., Zhao, D., et al. (2022). An integrated study of physical and numerical modelling on the stability of underground tunnel influenced by unloading rate. *Tunn. Undergr. Sp. Tech.* 129, 104602. doi:10.1016/j.tust.2022.104602
- Hao, X., Zhang, Q., Sun, Z., Wang, S., Yang, K., Ren, B., et al. (2021). Effects of the major principal stress direction respect to the long axis of a tunnel on the tunnel stability: physical model tests and numerical simulation. *Tunn. Undergr. Sp. Tech.* 114, 103993. doi:10.1016/j.tust.2021.103993
- Hoek, E., and Brown, E. T. (1988). “The Hoek-Brown failure criterion - a 1988 update,” in *Proc. 15th Canadian rock mech. Symp.* Editor J. C. Curran (University of Toronto), 31–38.
- Hoek, E., and Brown, T. (1980). *Underground excavation in rock*. London, Britain: The Institute of Mining and Metallurgy.
- Hoek, E., Marinos, P., and Benissi, M. (1998). Applicability of the geological strength index (GSI) classification for very weak and sheared rock masses: the case of Athens Schist Formation. *Bull. Eng. Geol. Env.* 57, 151–160. doi:10.1007/s100640050031
- Hu, T., He, S., Kang, Z., Tu, P., and Wang, D. (2023). Establishment and engineering application of viscoelastic-plastic constitutive laws for creep modeling in interbedded rock masses. *Sci. Rep.* 13, 20668. doi:10.1038/s41598-023-48003-w
- Jiang, Q., Feng, X.-t., Hatzor, Y. H., Hao, X.-j., and Li, S.-j. (2014). Mechanical anisotropy of columnar jointed basalts: an example from the Baihetan hydropower station, China. *Eng. Geol.* 175, 35–45. doi:10.1016/j.enggeo.2014.03.019
- Jiang, Q., Wang, B., Feng, X.-T., Fan, Q.-X., Wang, Z., Pei, S., et al. (2019). *In situ* failure investigation and time-dependent damage test for columnar jointed basalt at the Baihetan left dam foundation. *B. Eng. Geol. Environ.* 78, 3875–3890. doi:10.1007/s10064-018-1399-y
- Jin, C., Yang, C., Fang, D., and Xu, S. (2014). Study on the failure mechanism of basalts with columnar joints in the unloading process on the basis of an experimental cavity. *Rock Mech. Rock. Eng.* 48, 1275–1288. doi:10.1007/s00603-014-0625-6
- Lei, Y., Liu, Q., Liu, H., Chu, Z., Liu, P., and Wen, J. T. (2023). An updated Lagrangian framework with quadratic element formulations for FDEM. *Comput. Geotech.* 164, 105837. doi:10.1016/j.compgeo.2023.105837
- Li, A., Dai, F., Liu, Y., Du, H., and Jiang, R. (2021). Dynamic stability evaluation of underground cavern sidewalls against flexural toppling considering excavation-induced damage. *Tunn. Undergr. Sp. Tech.* 112, 103903. doi:10.1016/j.tust.2021.103903
- Li, A., Dai, F., Wu, W., Liu, Y., Liu, K., and Wang, K. (2022). Deformation characteristics of sidewall and anchorage mechanisms of prestressed cables in layered rock strata dipping steeply into the inner space of underground powerhouse cavern. *Int. J. Rock Mech. Min.* 159, 105234. doi:10.1016/j.ijrmms.2022.105234
- Li, A., Liu, Y., Dai, F., Liu, K., and Wei, M. (2020). Continuum analysis of the structurally controlled displacements for large-scale underground caverns in bedded rock masses. *Tunn. Undergr. Sp. Tech.* 97, 103288. doi:10.1016/j.tust.2020.103288
- Li, P. X., Chen, B. R., Xiao, Y. X., Feng, G. L., Zhou, Y. Y., and Zhao, J. S. (2023). Rockburst and microseismic activity in a lagging tunnel as the spacing between twin TBM excavated tunnels changes: a case from the Neelum-Jhelum hydropower project. *Tunn. Undergr. Sp. Tech.* 132, 104884. doi:10.1016/j.tust.2022.104884
- Li, T., Zhao, W., Liu, R., Han, J., Jia, P., and Cheng, C. (2024). Visualized direct shear test of the interface between gravelly sand and concrete pipe. *Can. Geotech. J.* 61 (2), 361–374. doi:10.1139/cgj-2022-0007

- Liu, G. F., Ran, G., Li, Z., Duan, S., Su, G., Yan, C., et al. (2023). An insight into the effect of primary hidden microfissures on mechanical behaviors and failure characteristics of brittle basalt. *Theor. Appl. Fract. Mec.* 128, 104138. doi:10.1016/j.tafmec.2023.104138
- Lu, B., Sheil, B. B., Zhao, W., Jia, P., Bai, Q., and Wang, W. (2024). Laboratory testing of settlement propagation induced by pipe-roof pre-support deformation in sandy soils. *Tunn. Undergr. Sp. Tech.* 146, 105645. doi:10.1016/j.tust.2024.105645
- Martin, C. D., Kaiser, P. K., and McCreath, D. R. (1999). Hoek-Brown parameters for predicting the depth of brittle failure around tunnels. *Can. Geotech. J.* 36, 136–151. doi:10.1139/t98-072
- Muller, G. (1998). Experimental simulation of basalt columns. *J. Volcanol. Geoth. Res.* 86, 93–96. doi:10.1016/S0377-0273(98)00045-6
- Saliba, R., and Jagla, E. A. (2003). Analysis of columnar joint patterns from three-dimensional stress modeling. *J. Geophys. Res.* 108, 1–7. doi:10.1029/2003JB002513
- Schultz, R. A. (1995). Limits on strength and deformation properties of jointed basaltic rock masses. *Rock Mech. Rock. Eng.* 28, 1–15. doi:10.1007/BF01024770
- Shi, A., Wei, Y., Zhang, Y., and Tang, M. (2020). Study on the strength characteristics of columnar jointed basalt with a true triaxial apparatus at the Baihetan Hydropower Station. *Rock Mech. Rock. Eng.* 53, 4947–4965. doi:10.1007/s00603-020-02195-z
- Si, X., Luo, Y., Gong, F., Huang, J., and Han, K. (2024a). Temperature effect of rockburst in granite caverns: insights from reduced-scale model true-triaxial test. *Geomech. Geophys. Geo-energy Geo-resour.* 10, 26. doi:10.1007/s40948-024-00736-2
- Si, X., Luo, Y., and Luo, S. (2024b). Influence of lithology and bedding orientation on failure behavior of “D” shaped tunnel. *Theor. Appl. Fract. Mec.* 129, 104219. doi:10.1016/j.tafmec.2023.104219
- Smith, J. V., and Holden, L. (2021). Rock slope kinematic instability controlled by large-scale variation of basalt column orientation. *B. Eng. Geol. Environ.* 80, 239–250. doi:10.1007/s10064-020-01917-5
- Wang, C., Liu, Y., Song, D., Xu, J., Wang, Q., and Zhang, S. (2024). Evaluation of bedding effect on the bursting liability of coal and coal-rock combination under different bedding dip angles. *Adv. Geo-Energy Res.* 11, 29–40. doi:10.46690/ager.2024.01.04
- Xia, K., Chen, C., Liu, X., Liu, X., Yuan, J., and Dang, S. (2023). Assessing the stability of high-level pillars in deeply-buried metal mines stabilized using cemented backfill. *Int. J. Rock Mech. Min. Sci.* 170, 105489. doi:10.1016/j.ijrmms.2023.105489
- Xia, K., Chen, C., Liu, X., Zheng, X., Zhou, Y., Song, X., et al. (2024). Ground collapse and caving mechanisms in strata overlying sublevel caving mines: a case study. *B. Eng. Geol. Environ.* 83, 21. doi:10.1007/s10064-023-03529-1
- Xia, Y., Zhang, C., Zhou, H., Chen, J., Gao, Y., Liu, N., et al. (2020). Structural characteristics of columnar jointed basalt in drainage tunnel of Baihetan hydropower station and its influence on the behavior of P-wave anisotropy. *Eng. Geol.* 264, 105304. doi:10.1016/j.enggeo.2019.105304
- Xu, H., Zhang, Z., Zhang, Y., Jiang, Q., Qiu, S., Zhou, Y., et al. (2024). Effects of natural stiff discontinuities on the deformation and failure mechanisms of deep hard rock under true triaxial conditions. *Eng. Fail. Anal.* 158, 108034. doi:10.1016/j.engfailanal.2024.108034
- Yang, G.-D., Wang, G.-H., Fan, Y., Deng, K., Lu, W.-B., and Zhao, J.-S. (2021). Dynamic response and performance of submarine tunnel subjected to surface explosions. *Mar. Struct.* 80, 103091. doi:10.1016/j.marstruc.2021.103091
- Zhang, J., Jiang, Q., Feng, G., Li, S., Pei, S., and He, B. (2022). Geometrical characteristic investigation of the Baihetan irregular columnar jointed basalt and corresponding numerical reconstruction method. *J. Cent. South Univ.* 29, 455–469. doi:10.1007/s11771-022-4940-x
- Zhao, J.-S., Chen, B.-R., Jiang, Q., Lu, J.-F., Hao, X.-J., Pei, S.-F., et al. (2022a). Microseismic monitoring of rock mass fracture response to blasting excavation of large underground caverns under high geostress. *Rock Mech. Rock. Eng.* 55, 733–750. doi:10.1007/s00603-021-02709-3
- Zhao, J.-S., Chen, B.-R., Jiang, Q., Xu, D.-P., He, B.-G., and Duan, S.-Q. (2024a). *In-situ* comprehensive investigation of deformation mechanism of the rock mass with weak interlayer zone in the Baihetan Hydropower Station. *Tunn. Undergr. Sp. Tech.*
- Zhao, J.-S., Duan, S.-Q., Chen, B.-R., Li, L., He, B.-G., Li, P.-X., et al. (2024b). Failure mechanism of rock masses with complex geological conditions in a large underground cavern: a case study. *Soil. Dyn. Earthq. Eng.* 177, 108439. doi:10.1016/j.soildyn.2023.108439
- Zhao, J.-S., Jiang, Q., Lu, J.-F., Chen, B.-R., Pei, S.-F., and Wang, Z.-L. (2022b). Rock fracturing observation based on microseismic monitoring and borehole imaging: *in situ* investigation in a large underground cavern under high geostress. *Tunn. Undergr. Sp. Tech.* 126, 104549. doi:10.1016/j.tust.2022.104549
- Zhao, J.-s., Jiang, Q., Pei, S.-f., Chen, B.-r., Xu, D.-p., and Song, L.-b. (2023). Microseismicity and focal mechanism of blasting-induced block falling of intersecting chamber of large underground cavern under high geostress. *J. Cent. South. Univ.* 30, 542–554. doi:10.1007/s11771-023-5259-y
- Zheng, Z., Li, R., and Zhang, Q. (2023a). A novel anisotropic deterioration mechanical model for rock ductile-brittle failure under 3D high-stress and its application. *Comput. Geotech.* 162, 105665. doi:10.1016/j.compgeo.2023.105665
- Zheng, Z., Tang, H., Zhang, Q., Pan, P., Zhang, X., Mei, G., et al. (2023b). True triaxial test and PFC3D-GBM simulation study on mechanical properties and fracture evolution mechanisms of rock under high stresses. *Comput. Geotech.* 154, 105136. doi:10.1016/j.compgeo.2022.105136